Peer-reviewed version available at Polymers 2020, 12, 1653; doi:10.3390/polym12081653

Review

Strength degradation in Curved FRP bars as Concrete Reinforcement

Thanongsak Imjai [1,*], Reyes Garcia [2], Maurizio Guadagnini [3] and Kypros Pilakoutas [3]

[1] School of Engineering and Technology, and Center of Excellence in Sustainable Disaster Management, Walailak University, Nakhonsithammarat, Thailand 80161; thanongsak.im@wu.ac.th
[2] School of Engineering, The University of Warwick, Coventry, UK CV4 7AL; reyes.garcia@warwick.ac.uk
[3] Department of Civil and Structural Engineering, The University of Sheffield, Sheffield, UK S1 3JD; m.gaugnini@sheffield.ac.uk (M.G.); k.pilakoutas@sheffield.ac.uk (K.P.)
* Correspondence: thanongsk.im@wu.ac.th; Tel.: +66-7567-2378

Abstract: Steel reinforcement in concrete has the tendency to corrode and this process can lead to structural damage. FRP reinforcement represents a viable alternative for structures exposed to aggressive environments and has many possible applications where superior corrosion resistance properties are required. The use of FRP rebars as internal reinforcements for concrete, however, is limited to specific structural elements and does not yet extend to the whole structure. The reasons for this relate to the limited availability of curved or shaped reinforcing elements on the market and their reduced structural performance. Various studies, in fact, have shown that the mechanical performance of bent portions of composite bars is reduced significantly under a multiaxial combination of stresses and that the tensile strength can be as low as 25% of the maximum tensile strength that can be developed in the straight part. In a significant number of cases, the current design recommendations for concrete structures reinforced with FRP, however, were found to overestimate the bend capacity of FRP rebar. This paper presents the state-of-the art review of the research works on the strength degradation in curved FRP composites and highlighted the performance of exiting predictive models for the bend capacity of FRP reinforcement. Recent practical predictive model based on the Tsai-Hill failure criteria by considering the material at marcromechanical level is also discussed and highlighted. The review also identifies the challenges and highlights the future directions of research to explore the use of shaped FRP composites in civil engineering applications and the trends for future research in this area.

Keywords: Curved FRP bars; bent fiber-reinforced polymer (FRP); bend capacity; bend strength; Bent test; strength & testing of materials; material characterisation.

1. Introduction

Since the late 1980s, Fibre Reinforced Polymer (FRP) reinforcement has emerged as an alternative to replace conventional steel bars in reinforced concrete (RC) structures [1]. Since FRP reinforcement does not corrode and is more durable, it can extend the structures' service life and reduce maintenance/repair costs in concrete structures [2]. To date, internal FRP reinforcement for concrete is mainly limited to specific structural applications such as bridge decks, road barriers, marine structures, and tunnel and underground infrastructure. The limited use of internal FRP reinforcement can be partly due to the lack of commercially available curved or shaped reinforcing elements needed for complex structural connections [3][4].

Peer-reviewed version available at Polymers 2020, 12, 1653; doi:10.3390/polym12081653

In current construction practice, most of the curved/shaped steel bars are pre-bent and cut off-site. Unlike FRP reinforcement, steel bars have an elastoplastic behavior and therefore they can be easily shaped by cold bending. Existing guidelines for the cold bending of steel bars (e.g. BS 8666 [5]) specify a bend radius to diameter ratio (r/d) of 2 for mild steel, which would induce a maximum strain value of 20% in the steel (see Figure 1). In the case of cold-bent FRP reinforcement, however, there are problems associated with the potential buckling of the fibres located on the compression side. Moreover, the typical ultimate strain value of FRP products varies from 1% to 2.5%, hence, the induced strain in the fibres needs to be controlled to avoid premature failure of the reinforcement. As a result, cold bending of FRP reinforcement requires larger r/d ratios than those currently specified for steel reinforcement.

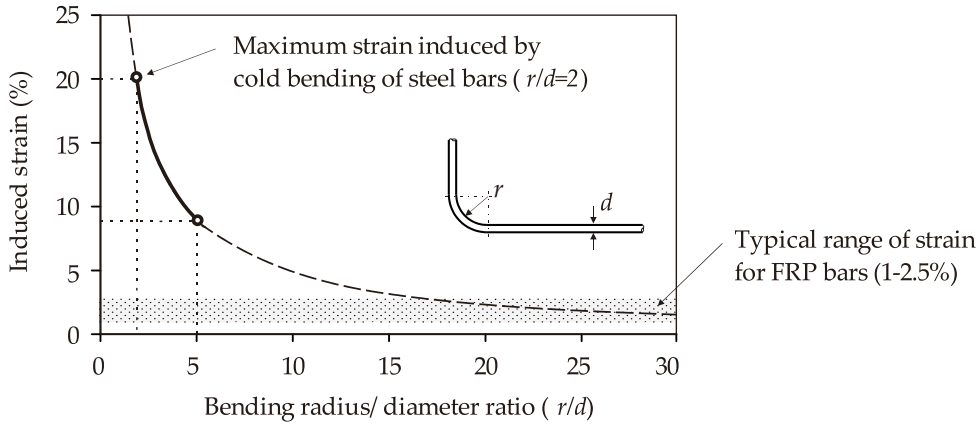

Figure 1. Induced strain values in cold bent bars (adapted from Imjai et al. [6])

To date, only a few of the FRP bars commercially available are supplied in bent configurations, and all of them are pre-bent during manufacturing. Bends are usually created while the material is partially cured. Typical bent shapes available include: closed stirrup of thermoplastic FRP strip (Figure 2a), J-hook thermoplastic FRP strip, pre-bent GFRP thermoset composite (Figures 2b and 2c), and U-shaped thermosetting FRP bar (Figure 2d). Whilst Carbon (CFRP), Glass (GFRP), Aramid (AFRP) and basalt (BFRP) bars exist in the market, CFRP and GFRP seem to be much more widely used in actual RC applications and research. CFRP has better properties than all the other composites, whereas GFRP is significantly cheaper than other composites.

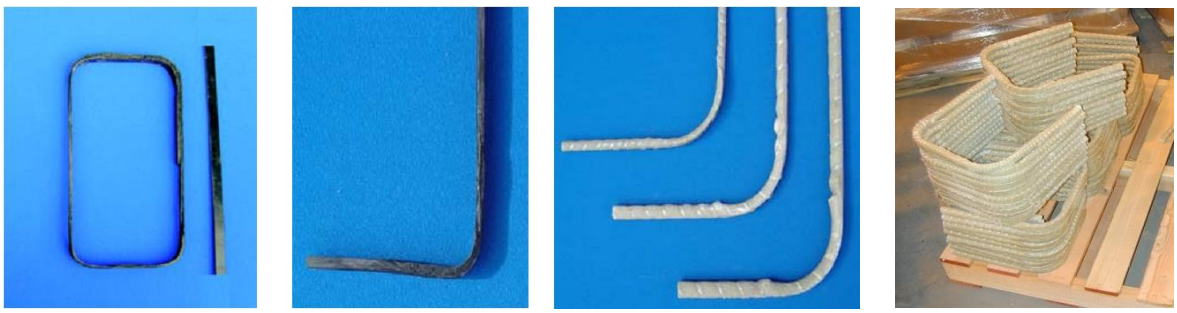

(a) (b) (c) (d)

Figure 2. Commercially available curved FRP reinforcements: (a) closed stirrup FRP strip, (b) J-hook FRP strip, (c) pre-bent FRP bar, and (d) U-shaped FRP bar [3]

Whilst FRP materials work most effectively when subjected to pure axial tension, most FRP RC structures are subjected to a combination of stresses. Previous studies have reported that the tensile strength of FRP reinforcement reduces under a combination of tensile and shear stresses [6]–[18]. This becomes an issue in curved FRP reinforcement in RC structures since premature failures can occur at the bent corner. Research has shown that the tensile strength of a bent portion of a FRP bar can be as low as 25% of the maximum tensile strength of that developed in the straight part. The strength

degradation occurs at the bent portion of an FRP bar can be quantified using empirical equations such as the one initially proposed by the Japanese Society of Civil Engineering (JSCE) [10] which is currently adopted in many design guidelines for the use of FRP reinforced concrete structures. To account for this potential failure, several design guidelines ([19][10], [20]–[22]) limit the design strain values in the case of curved FRP reinforcement in reinforcement concrete structures. However, equations included in the current design guidelines to predict the bend strength degradation at the bent portion of an FRP bar is an empirically derived equation which is mainly a function of bent geometry and does not seem to yield consistent results when different types of composite are used [23].

This article provides an overview of existing and ongoing research on the strength of curved FRP reinforcement in RC structures. Extensive experimental works to investigate the strength degradation of curved FRP composites are systematically presented and test data available from literature is also included in Appendix as an additional source. Modern techniques used to fabricate customized/ complex shaped FRP composites are also discussed as emerging challenges.

3. Research on strength degradation of curved FRPs

Although extensive work has examined the behaviour of RC structures internally reinforced with FRP, relatively little information is available on curved FRP reinforcing bars [24]–[26]. These studies focused on determining the "*bend capacity*" of curved FRP reinforcement using pullout test on bent FRP bars embedded in concrete specimens (Figure 3). Different test configurations were used in examining the bend capacity of FRP bars, as summarised in the following paragraphs.

Ozawa et al. [24] tested studied the static and flexural fatigue behaviour of concrete beams reinforced with FRP flexural and shear reinforcement, consisted of continuous glass and carbon fibres impregnated with resin and formed by the filament winding method. A total of 10 beam specimens were tested under two-point bending; two of them were statically loaded and the other eight were fatigue loaded. The authors reported that, if the beams failed in shear, FRP stirrups could fail at the bent portion at a stress lower than the ultimate strength of the equivalent straight bar. Ozawa et al. concluded that the stress concentration that developed at the bent portion of the bar caused rupture, a failure which originated from the inside of the bend. Similar conclusions were also reported by Miyata et al. [25] after carrying out a series of pull-out tests that studied the effect of bends on hybrid FRP bars embedded in concrete blocks (see Figure 3a). Direct tensile tests were performed on the reinforcement, which consisted of a 10 mm-diameter hybrid FRP composite made of continuous glass and high strength carbon fibres impregnated with resin. The main parameter investigated was the variation of the tensile strength of bent FRP bars as a function of the internal bending radius (r). Five different bar diameters were used in the test and bending radius was set to three times the bar diameter (i.e. $r/d=3$). The authors reported that most of the bent specimens failed due to the rupture of the FRP bars at the bent section, and that the fibres started to break from the inside portion of the bend. They also concluded that the failure load increased as the internal bending radius increases. Although the studies by Ozawa et al. [24] and Miyata et al. [25] provided some insight into the strength degradation of bent FRP bars, the tests only considered a few test parameters and therefore their conclusions were not generalised. However these tests did not consider the bond contribution along the bent portion and the effect of tail anchorage. Other parameters that could affect the bond stress such as concrete strength and surface treatment of FRP bars were also excluded in this test.

Peer-reviewed version available at Polymers 2020, 12, 1653; doi:10.3390/polym12081653

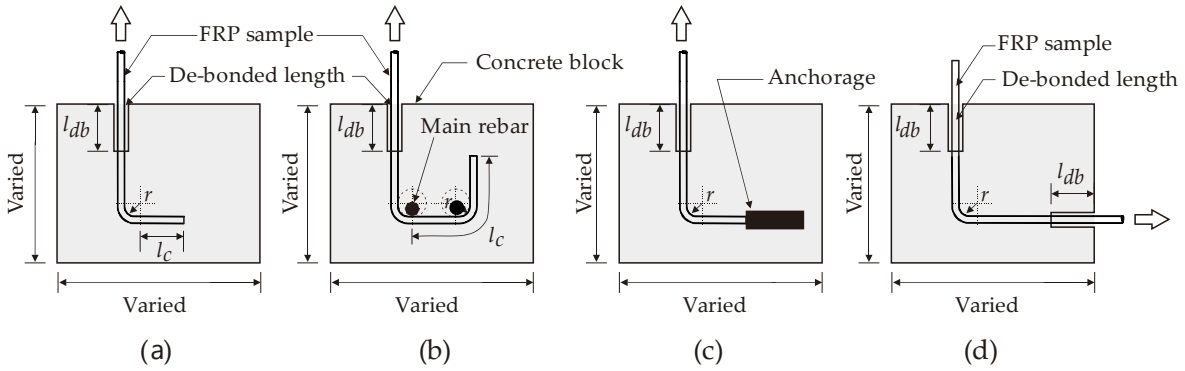

Figure 3. Different pullout setup for examining the bend capacity of FRP reinforcement (illustration adopted from [25], [12], [8], [11])

To examine the factors that influence the shear capacity of concrete beams contributed by FRP stirrups, Nagasaka et al. [12] tested 35 half-scale beams internally reinforced with FRP bars. Parameters investigated were the type and reinforcement ratio of FRP stirrups, as well as the concrete strength. Nagasaka et al. also tested four panel specimens to investigate the bend capacity of the FRP stirrups with the main reinforcement to simulate the bond at the bent location around the main bar, using the pullout arrangement shown in Figure 3b. The FRP bars were aramid, carbon, glass, and hybrid of glass and carbon FRP. The vertical leg was left unbonded to the beginning of the bent portion and the bend radius was 2 times the bar diameter (r/d=2). They reported that the ultimate shear capacity of concrete beams reinforced with FRP stirrups was determined by the tensile rupture of stirrups at the curved sections, or by crushing of a concrete strut formed between diagonal cracks. They also found that the tensile strength of curved FRP bars was only 25%-80% of that of a straight counterpart. One of the main contributions of Nagasaka et al. study is that the degree of bend capacity reduction depended on the type of composites.

Similar tests were carried out by Maruyama et al. [8] who tested 14 bent FRP samples embedded in concrete blocks with a 50 mm embedment length, l_{db} and the anchor at the end of tail to improve the bond stress (Figure 3c). The main parameters studied were different types of composite materials, bending radii, and concrete strength. Curved pultruded CFRP rods, 7-strand CFRP rods, and braided AFRP rods were tested in direct tension and compared to steel bars with similar configurations. The bending radii (r) considered in this study were 5, 15, and 25 mm for each type of rod. Two different concrete strengths were used; ($f'_c = 50\ MPa$ and $100\ MPa$) for each type of FRP rods. It was reported that all of the specimens failed due to rupture of the composite at the beginning of the bend on the loading side and all of the bend capacity of FRP bars were found to be lower than the tensile strengths of the straight portions, ranged from 48-82%. Moreover, the bend capacity trended to decrease hyperbolically as the bending radius decreased, and the bend capacity of FRP specimens were increased when the higher strength concrete was used and became more pronounced with 7-strand CFRP rods, and braided AFRP rods. This may be due to better bond developed by the stranded and braided composites, and the resulting lower amount of tensile stress transferred to the bend. In case of pultruded CFRP rods, the concrete strength had little effect on the bend capacity. This may be because the bond given by the roving wrapped around the rod was lost during the pullout tests, and thus adhesion at the bar-concrete interface becomes less significance. The authors also reported that the tensile strength at the bend varies with the type of fibre and the method of bending. The highest bend capacity-to-strength ratio was mobilized by braided AFRP rods, followed by strand CFRP and pultruded CFRP rods. These results indicated that the bend capacity depeneded on the type of FRP and the reinforcement surface (i.e. on bond properties). It should be mentioned that the test results of Maruyama et al. [8] were later used to validate the predictive equation for calculating the bend capacity of FRP reinforcement which is referred as the JSCE's equation [10] and now included in the current ACI guidelines [27] used to predict the bend strength of FRP bars.

Ehsani et al. [11] investigated the bond behaviour of 90° degree-hooked GFRP bars in concrete through thirty-six direct pullout tests as those shown in Figure 3d. The main parameter examined in Ehsani et al.'s study was the relationship between the strength capacity of curved FRP bars and the concrete compressive strength (f'_c), which varied between 28 MPa and 56 MPa. Other examined parameters included bend radius to FRP bar diameter ratio (r/d= 0,3) (diameters, d= *9.5, 19.0, 28.6* mm), embedment length, and tail length (l_c) beyond the hook. In these tests, the tensile load was horizontally applied through a gripping system (Figure 3d). Ehsani et al. found that the bend capacity was highly affected by the bend radius and bar diameter. When using r/d=*3*, the bend capacity ranged from 64% to 70% of the ultimate tensile strength and the bend capacity trends to increase when higher concrete strength was used. Based on their results, the authors recommended a minimum bend radius of *3d* for GFRP hooks, as well as a tail length of *12d* since the tail length beyond *12d* had no beneficial effect on the strength of the bent bar. As the bend capacity increased with the embedment length, Ehsani et al. also recommended a minimum development length of *16d* for a 90° standard GFRP hook. The results from this study confirmed that concrete strength, embedment length and tail length are important parameters that influence the bent portion of FRP bars. Unfortunately, the studies by Ehsani et al. [11] did not consider types of composite used as well as different bending geometries that could affect the bend capacity of FRP bars.

The effectiveness of bent FRP reinforcement depends on the bond characteristics of the reinforcement itself, but also on the characteristics of the embedment and tail lengths. Accordingly, Vint and Sheikh [6] examined the bond performance of GFRP bars with different anchorage configurations (90° degree-hooked bars and straight bars with mechanical anchor heads). 72 pullout GFRP specimens (as shown in Figure 3b) were tested using different anchorage configurations: straight anchorage, mechanical anchor heads or bends. Bent GFRP bars with different bending radius and surface coatings were used to examine the performance of this anchorage solution. Vint and Sheikh concluded that the full tensile strength in the fibre direction could be developed for bonded lengths of 5*d* in specimens with bent bars, and 10*d* for specimens with an anchorage head. However, the bend capacity of the GFRP bars was only 58-80% of the ultimate tensile strength of the straight portion. This indicates that, although mechanical anchor heads can potentially enhance the bond behavior of bent FRP bars, the theoretical ultimate tensile strength of the bars could not be achieved. The above mentioned studies examined the bend capacity of FRP bars using geometries typical of end anchorages (e.g. relatively large corner radius) However none of the previous studies tested FRP reinforcement with geometries similar to those used in steel stirrups.

Previous research also studied the effect of bends in FRP stirrups, but using geometries similar to those used in conventional steel stirrups [28][13], [16], [23], [29]–[37]. In these conditions, the tight corner radius of FRP stirrups tend to limit the shear capacity of the concrete beams where premature failure was generally observed at the proximity of the bent portion. To study the failure behaviour of thermoplastic FRPs as shear reinforcement in concrete beam, bent tests on thermoplastic FRP stirrups were nylon/carbon and nylon/aramid FRP fibres formed using a thermoplastic matrix resin in the pultrusion process was investigated by Currier et al. [38]. Thermoplastic FRP strips were bent in the laboratory by the application of heat to create the closed shape of shear links, having the internal bending radius of 12.7 mm and the bend capacity of the thermoplastic FRP links were evaluated using the test setup similar to the ACI B.5 method. Based on their test, the bend capacity of the thermoplastic FRP bars was 25% of the ultimate tensile strength of the straight portion and the failure on all of the tested specimens were observed at the bend portion of the stirrup.

Initial research by Ueda at al. [30] investigated the performance of FRP stirrups partially embedded into a concrete block, which aimed to simulate a shear crack crossing the FRP stirrups. The 6 mm-diameter FRP rods used in Ueda at al.'s study were braided epoxy-impregnated aramid fibres. The main variables in the study were the embedment length and the distance from the artificial crack to the bend. Tensile forces were transferred through steel plates, and steel rods to the bearing plates. The test setup was adopted from the ACT B.5 method (e.g. Figure 5a), except the free distance between two concrete blocks was not 200 mm but using the artificial crack instead. An artificial crack initiated with a 0.5 mm gap began to open and the tensile forces were then induced in the bent

portions of the FRP sample. Ueda at al. also conducted Finite Element Analyses (FEA) to assess the nature of the stress-strain fields developed in the bent region. Their results showed that the bend capacity varied between 40% to 100% of the ultimate capacity in the direction of the fibres. The FEA showed that high strains developed in the inner portion of the bend, which was assumed as the location of failure initiation. For an embedment length of 100 mm, the failure stress was higher than the nominal strength of the straight bar. Accordingly, the numerical analysis performed by Ueda at al. was perhaps the first who attempted to investigate the stress-strain field at bent portion of FRP bars and the results agreed with the previous research where premature failure mostly initiated at the proximity of the bends.

Morphy et al. [18] tested sixteen specially-designed specimens using different types of FRP stirrups using the ACI B.5 method [39] as shown in Figure 5a. Parameters investigated were the type of FRP material, bar diameter, stirrup anchorage and embedment length of the stirrup into the concrete and the configuration of the stirrup anchorage. Three types of FRP reinforcement were used: Carbon FRP Leadline bars, Carbon Fibre Composite Cables (CFCC), and GFRP bars (C-BAR). All of the bent stirrups were embedded in concrete blocks with $f'_c = 45\ MPa$. The embedment length within the block varied by debonding part of the stirrups. The authors found that a decrease in the embedment length increases the tendency of failure at the bent region of the stirrup, which resulted in a bend capacity of 40% of that developed in a straight bar. From the results, it was suggested that a 150 mm embedment length was sufficient to achieve the full strength in the direction of the fibres. Morphy et al. also found that when a large bending radius to bar diameter ratio (r/d) is used, a higher bend capacity was observed. Based on their test results, and using the stirrup spacing recommended by the ACI codes [40], they proposed to limit the strength of CFRP stirrups to 50% of the unidirectional tensile strength to account for the strength degradation due to bend effect.

More recently, Imjai et al. [6] studied of the bend capacity on bent FRP stirrups using the pullout test shown in Figure 4a. 47 bent thermoset and thermoplastic FRP bars with 19 different configurations were investigated. The parameters investigated included the ratio r/d, surface treatment, embedment length (l_b) and concrete strength (f'_c). It was found that the capacity of the curved FRP composites could be as low as 25% of the ultimate tensile strength of the material parallel to the fibres. Based on the results, it was recommended to use a minimum ratio $r/d=4$ to guarantee that the composite could resist 40% of its unidirectional tensile strength parallel to the fibres. Imjai et al. also conducted FEA to study the bond stress along the bent portion of FRP bar embedded in concrete. The bond mechanism between the bent bar and the concrete was explicitly modelled with identical non-linear spring elements with the stiffness determined from the load-slip characteristic from the pullout tests. The FEA results confirmed that high stress concentrations develop at the beginning of the bent portion, thus indicating that failure could be expected to occur at this location (Figure 4c). However, by using a larger bending radius or providing sufficient bond along the bent portion, the stress concentration at the beginning of the bend can be significantly reduced, and a higher bend capacity can be achieved.

Preprints (www.preprints.org) | NOT PEER-REVIEWED | Posted: 22 July 2020 doi:10.20944/preprints202007.0524.v1

Peer-reviewed version available at Polymers 2020, 12, 1653; doi:10.3390/polym12081653

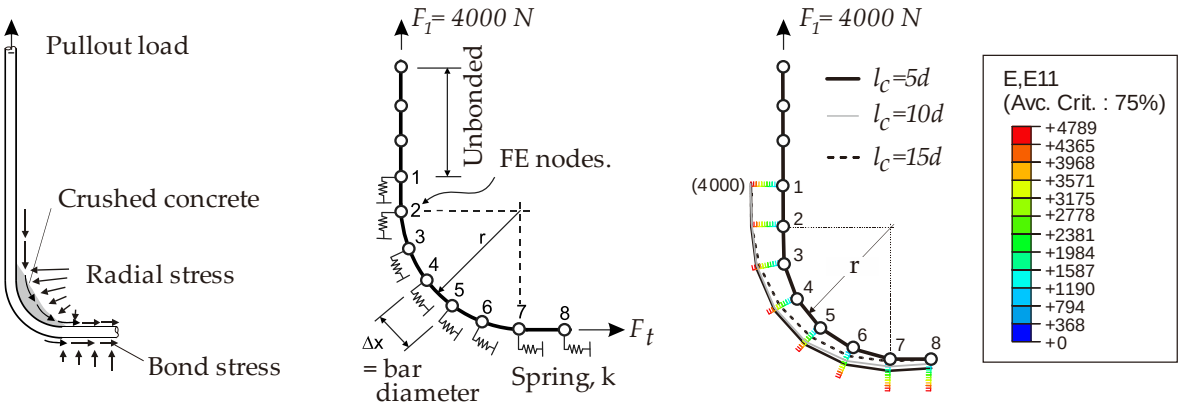

Figure 4. Physical model vs Mathematical FE model for a bent FRP bar from Imjai et al. [6]

Although all of the experimental works mentioned above have dealt with the study of the behaviour of curved FRP bars embedded in concrete structures such as stirrups or anchorages, externally bonded FRP reinforcement (EBR), which have gained widespread use as strengthening material for RC structures in order to provide confinement and/or shear capacity may also suffer the bent effect, especially when bending the fibres over the member corners. The need for bending the composites may deteriorate the performance of the FRP laminate and the efficiency of its confining/strengthening action. Yang et al. [41] studied the effects of corner radius on the strength of FRP lamina using the test setup similar to the ACI B.12 [39]. In their experimental programme, one and two plies CFRP lamina were applied by the manual lay-up procedure over interchangeable corner inserts. They concluded that the corner radius (r) affects the strength of CFRP laminates. The test results showed that only 67% of the ultimate laminate strength could be developed when a large radius of insert was used. As the corner radius was decreased, the strength capacity of the FRP lamina further reduced. A higher failure stress was achieved by increasing the number of layers used.

Based on the literature summarized in this section, it is evident that numerous factors affect the bend capacity of FRP reinforcement such as bent geometry, materials of which type of composite is made, concrete strength, and bond stress between concrete/FRP bar interface. Advanced FE technique were used to study stress-strain field along the bent portion of FRP bars and the results confirmed that premature failure always initiated at the proximity of the bends which confirmed the reports from companion works from literature. However, issues such as mechanics at macro-scale of the material composition of composite bent portion when subjected to external loads, irregular shape and cross-section and bond stress along the bent portion have not been investigated yet and are a matter of future research. The results from the tests discussed in this section have also been reflected in the development of the predictive equation to the current design guidelines, as discussed in the following section.

4. ACI test methods of determining bend capacity of FRP bars

Different tests have been proposed to calculate the strength reduction in bent bars. The test rigs applicable to FRP bars for use in nonprestressed concrete outlined in ACI 440.3R [39] includes the B.5 method (bent bar capacity) and the B.12 method (corner radius), and these are illustrated in Figure 5a and b, respectively. The *B.5 method* measures the ultimate capacity of the FRP by testing (in tension) the straight portion of a FRP C-shaped stirrup whose bent ends are embedded in two concrete blocks (Figure 5a). The bend capacity of bent FRP bars are measured and compared to the ultimate tensile strength of the bar to obtain the strength reduction factor due to bend effects. The *B.12 method* measures the effect of the corner radius on the tensile strength of the FRP bar using a the testing

Preprints (www.preprints.org) | NOT PEER-REVIEWED | Posted: 22 July 2020 doi:10.20944/preprints202007.0524.v1

Peer-reviewed version available at Polymers 2020, 12, 1653; doi:10.3390/polym12081653

apparatus shown schematically in Figure 5b. The apparatus applies tension in the U-shaped FRP that reacts against the bent portion mounted on a yoke.

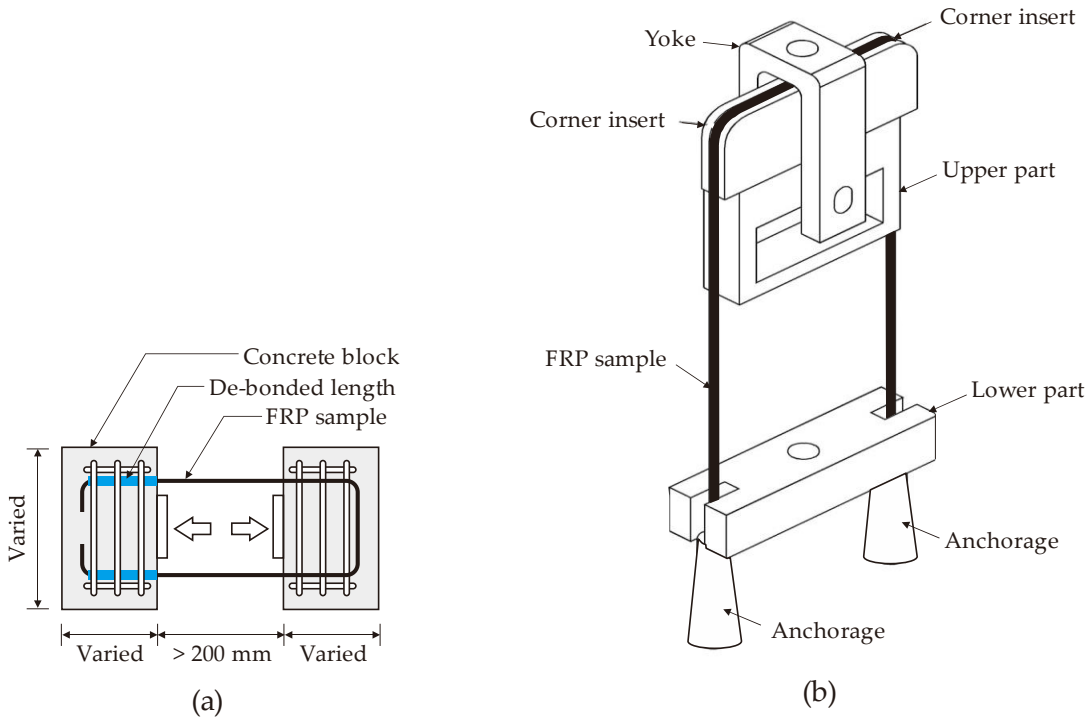

Figure 5. ACI test method; (a) B.5 and (b) B.12 (Adopted from ACI 440.3R [39])

In North America, ISIS Canada [42] and ACI 440.6M-08 [43] suggest using either ACI B.5 or B.12 to determine the bend capacity of curved FRP reinforcement. Ahmed et al. [16] conducted both the ACI B.5 and B.12 tests on 4 CFRP stirrup specimens, and 12 GFRP stirrup specimens, respectively. Ahmed et al. concluded that the B.5 test method led to more realistic results in evaluating the bend capacity of the FRP stirrups because the test arrangement simulates better the actual mechanism of stirrups embedded in concrete.

Based on the review in this section, it is evident that the guidelines provide two standard test configurations to assess the bend capacity of FRP reinforcement and the ACI B.5 method was mostly adopted in the test setup with the purpose of examining the bend strength of FRP composite as shear reinforcement embedded in concrete member. On the other hand, the ACI B.12 method led to more realistic results when FRP composite was applied externally on the concrete members such as strengthening works and the ACI B.12 method will led to a conservative result where bond between FRP-concrete is not considered for such applications. However, a simple pullout test to examine the bend capacity of FRP composites has been widely used in the literature due to the fact that the setup can be practically conducted and parameters such as bent geometry, embedment length and tail length could be easily installed in the setup whereas the ACI B.5 and B12 methods require more details in the test setup and eccentricity of the applied loads has to be carefully monitored. The results of the bend tests performed by several test methods in the literature were used in the process of the development of the predictive model for the bend capacity and will be described in detail in the following section.

5. Models to assess the bend capacity of FRP reinforcement

Chronological development of predictive model for bend capacity and code provisions is shown in Figure 6. In 1995, Nakamura and Higai [17] conducted a theoretical study on the bend capacity of FRP stirrups based on test results from Miyata et al. [25]. As a result of their study, the authors proposed an empirical model to calculate the bend capacity of FRP composites (f_b) as shown in Table 3; Equation (1). The model depends primarily on the bend ratio r/d, and therefore neglects the variation of the composite cross-section, the type of composites and the influence of bond characteristic between FRP/concrete interface.

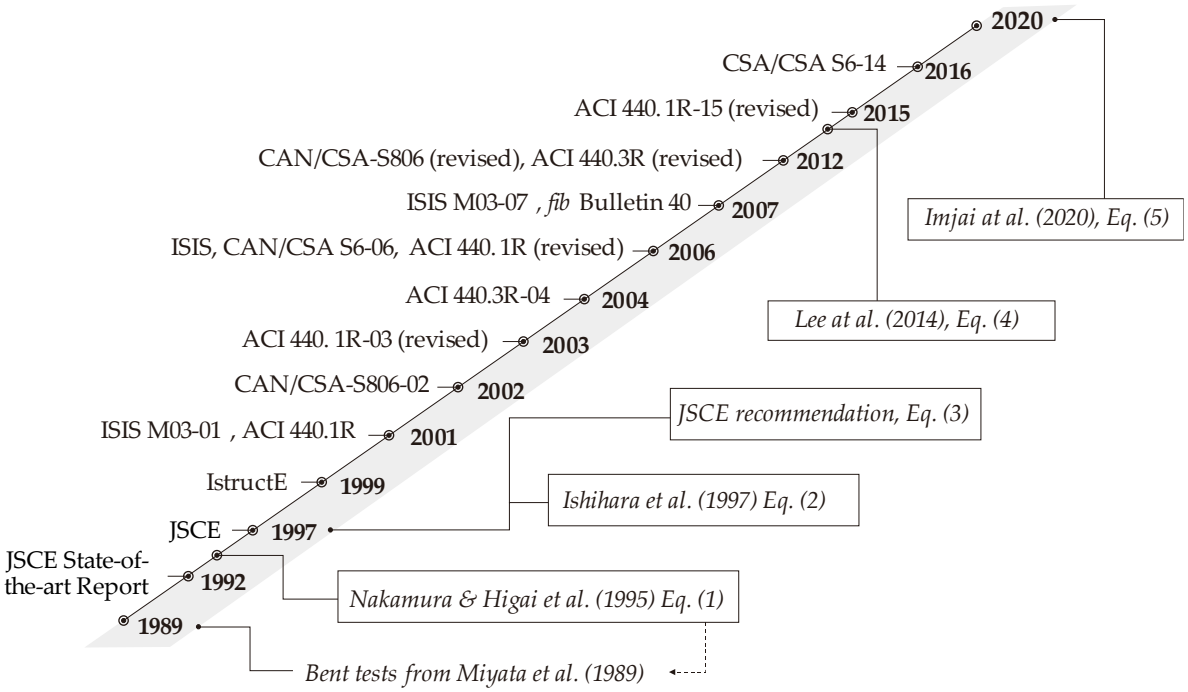

Figure 6. Chronological development of predictive model for bend capacity and code provisions

Based on test results from Ueda et al. [30], Ishihara et al. [15] analysed the behaviour of bent FRP stirrups embedded in concrete using a 2D FEA. The results of their study showed that the strength of a bar at its bent portion increases directly with the radius of the bend. Based on a FEA parametric study, Equation (2) was proposed to assess the strength of the bent portion (f_b). Note that Equation (2) is a special case of Equation (1) in which λ replaces d/r. The study by Ishihara et al. showed that the reduction in bend strength was also a function of the different types of FRP composites. Ishihara et al. suggested that bond characteristics and differential slippage of the FRP rod (which were not considered in their FEA) could play an important role in the strength reduction.

Figure 7a and b compare, respectively, the predictions given by Equations (1) and (2) and test data from Miyata et al. [25] and Ishihara et al. [15]. The results show that the experimentally derived bend capacity increases with increasing r/d ratio. Figure 7a also shows that the predictions from Equation (1) agree better with the test results when compared to Equation (2). This is not surprising as Equation 1 was empirically derived using test data from Miyata et al. [25]. In Figure 7b, it can be observed that Equation (2), as proposed by Ishihara et al. [15] predicts the experimental results more accurately than Equation (1). This is because the equation proposed by Ishihara et al. [15] was empirically derived using their own test data.

Preprints (www.preprints.org) | NOT PEER-REVIEWED | Posted: 22 July 2020 doi:10.20944/preprints202007.0524.v1

Peer-reviewed version available at Polymers 2020, 12, 1653; doi:10.3390/polym12081653

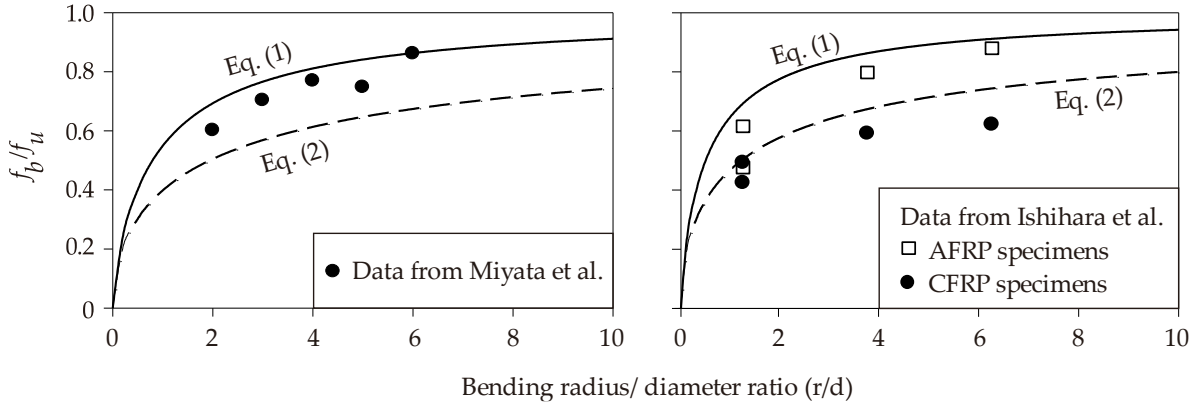

Figure 7. Predicted bend capacity of FRP bars from Nakamura and Higai (a) and Ishihara et al. (b) models

The strength degradation at the bend portion of FRP composite has been quantified using the predictive model (Equation (3)) included in current design recommendations for concrete structures reinforced with FRP composite materials (see Table 1) [44][20], [22], [43], [45] which is based on the original work by the JSCE guidelines [10]. In Equation (3), the strength of the bent portion, f_b, is expressed solely as a function of the uniaxial tensile strength of the composite, f_u, and the bar geometry (i.e. bar diameter, d, and bend radius, r). The strength of the bent portion varies greatly even for the same type of fibres, depending on the bending characteristics, and type of resin used. Therefore, the strength of the bent portion should be determined on the basis of suitable tests. The regression line in Figure 8 is supposed to give an adequate margin of safety. It should be noted that Equations 1 to 3 are only applicable to circular FRP bars.

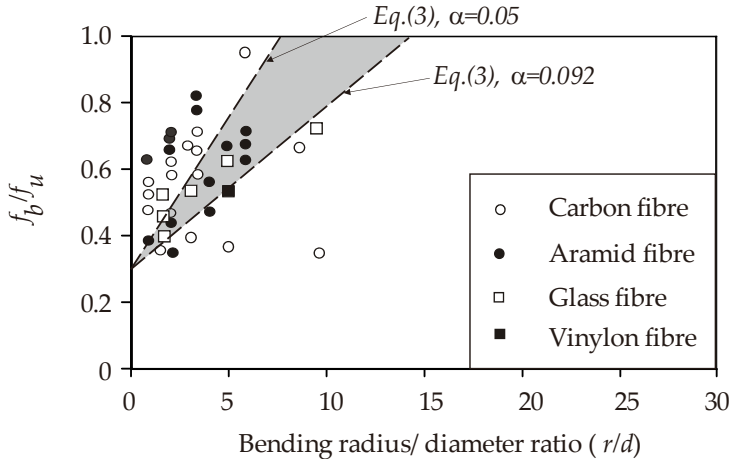

Figure 8. Bend capacity by JSCE's equation (adapted from JSCE document [10])

More recently and based on modifications to Equation (3), Lee et al. [13] proposed Equation (4) to calculate the bend capacity of non-circular FRP sections. Non-circular bars are converted into equivalent circular bars using an equivalent diameter with the safety factor (Fs). The safety factor Fs is given different values, such as Fs =1.3 in JSCE [10] and 1.5 in ACI440.1R-15 [27] , CAN/CSA S6-06 (CSA 2006), and ISIS-M03-07 [45]. Lee et al. also proposed different values of α (suitable for Equation (3)) using linear regression analysis from 14 tests. The researchers also validated their model (Equation 4) using previous ACI B.5 bent test data from the literature [14], [16], [29].

It should be noted that Equations (1-4) are empirical and only depend on the geometry of the bend, whilst the bond characteristic between FRP bar/concrete interface, type of FRP and material composition are neglected. Recent research by Imjai et al. [23] demonstrated that the predictions of Equations 1-4 do not match the experimental data available in the existing literature. As a result, Imjai et al. proposed a new macromechanical-based equation (Equation 5) that calculates more accurately the bend capacity of bent FRP reinforcement. Equation 5 adopts the Tsai-Hill failure criterion [46] for a unidirectional orthotropic lamina with fibres in the one-direction and subjected to plane stress in the 1-2 plane. The bend capacity (f_b) was expressed as a function of the strength reduction factor (k) multiplied by the ultimate strength parallel to the fibres (f_u). The strength reduction factor (k) is less than unity and ranged from 0.25 – 0.70, depending on the value of β. The factor β (ratio of the longitudinal tensile strength and transverse compressive strength of the FRP material). In their model, the factor β was explicitly derived from the Tsai-Hill failure criterion which represents the physical meaning of materials at the macro-scale and type of composite/resin composition is being considered when determining the bend capacity of unidirectional FRP composites.

1

Table 1. Summary of equations to predict the strength degradation of curved FRP reinforcement

References		Remarks
Nakamura and Higai [17]		
$f_b = \frac{r}{d}\ln\left(1+\frac{d}{r}\right).f_u$	(1)	Empirical model derived using test data from Miyata et al. [25]
Ishihara et al. [15]		
$f_b = \frac{1}{\lambda}\ln(1+\lambda).f_u$	(2a)	Derived using test data from Ishihara et al. [15] and further compared to the numerical results obtained from a 2D FE analysis
where $\ln\lambda = 0.90 + 0.73\ln(d/r)$	(2b)	
JSCE [10]		
$f_b = (\alpha\frac{r}{d} + 0.3)f_u$	(3)	Empirical model based on test results performed by the Japanese researchers. Unfortunately, information on these tests is not available for all of specimens and only selected test data from JSCE extracted from Ishihara et al. [15] are presented in the Appendix
Lee et al. [13]		
$f_b = \frac{\left[0.02\left(\alpha\frac{r}{d_{fi}} + 0.47\right).f_u\right]}{F_s}$	(4)	Eq. (4) is a modification of Eq. (3) but the former can be applied to of non-circular sections. Model uses the diameter of the equivalent circular section by converting non-circular bars to equivalent circular bars, d_{fi}. α values were obtained from linear regression analysis from 14 tests.
Imjai et al. [23]		
$f_b = k.f_{fu}$	(5a)	Model adopts the Tsai-Hill failure criterion for a unidirectional orthotropic laminar composite at a macroscopic level and considers force equilibrium at bent zone. Model calibrated using test results from 26 tests [6] and subsequently verified against 54 tests results available in the literature.
where $k = \frac{1}{\sqrt{1+\left(\xi.\frac{1}{r}\right)+\left(\xi.\frac{1}{r}\right)^2\beta^2}}$	(5b)	

f_b = bend capacity, f_u = ultimate strength parallel to the fibres, r = bend radius, α =0.05 corresponds to a 95% confidence limit, and α =0.092 corresponds to a 50% confidence limit, d = nominal diameter of the bars, *dfi* = diameter of the equivalent circular section, F_s = is the safety factor, $\xi = \frac{\pi d}{4}$ or t for circular or rectangular cross-sections, respectively, β = strength ratio, and k = strength reduction factor for bent FRP bars

2

6. Comparison of models for bend capacity of FRP reinforcement

This section compares the accuracy of the equations shown in Table 1 against test data available in the literature (summarised in Appendix A). In Equation 5, the strength reduction factor k used in the calculations depends on the parameter β, which is the ratio of the longitudinal tensile strength (f_u) and the transverse compressive strength (f_{cT}). The values of f_{cT} were not available for any of the composite specimens summarised in Appendix A. Accordingly, a value $\beta=7.5$ is recommended as the back-calculation of the transverse compressive strength was in the range *80–246 MPa*, which lies within the typical range for FRP composites reported in the literature [23].

Figure 9 compares 80 test results from the literature and results calculated with the equations in Table 1. The comparative results presented in Figure 9 shows clearly that the JSCE's equation ($\alpha=0.05$) is conservative, with a mean prediction/experiment ratio $P/E = 1.02$, and a standard deviation $SD =0.27$. It can be also seen that the five equations yield quite different ranges of results. For instance, Equations (1) and (2) overestimate the bend capacities for the data in the literature, as shown by a $P/E=1.66$ *and* $SD=0.46$ for Equation (1), and $P/E=1.34$ *and* $SD=0.33$ for Equation (2). In comparison, Equation (4) predicts better the test results and has less scatter ($P/E=1.08$, $SD=0.28$). Equation (5) shows the best agreement with the test results and has a low scatter ($P/E=1.00$, $SD=0.25$). The differences between the calculated values can be attributed to differences in the original formulation of the empirical equations could be attributed to the influence of the types of composites used in the experimental programme.

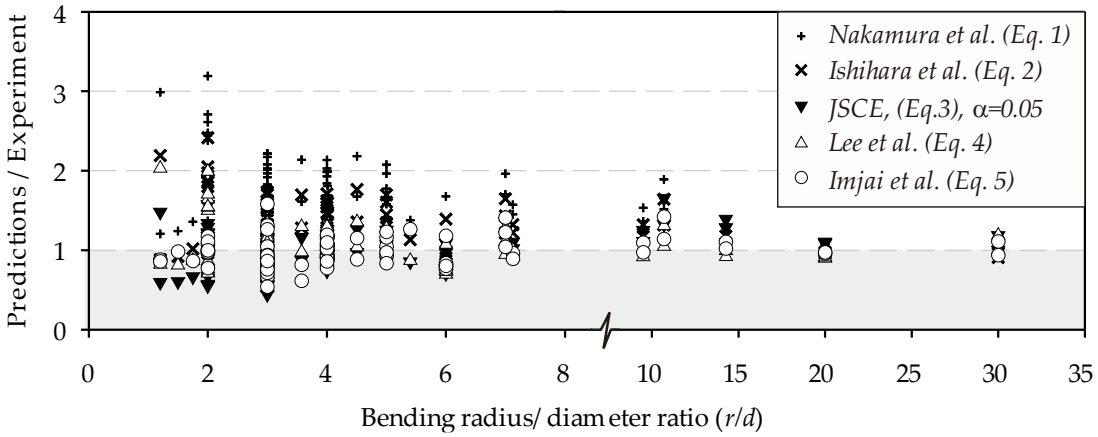

Figure 9. Prediction of experimental tests using existing code provision and models

7. Prefabricated FRP composites and Future Challenges

In the past, the methods to manufacture complex or customized FRP shapes were very expensive and required complicated manufacturing process. Nowadays, with the aid of computer automatic control and 3D printing, various shaped FRP reinforcements shown in Figure 10 are currently available in the construction market. Advanced filament winding manufacturing process has been developed in which resin-impregnated fibres are wound onto specially-designed mandrels to produce customized closed shapes such as shear stirrups. In these pre-bent closed loop stirrups, the material is wound around a mould into one large stirrup. After the completion of the curing process, the mould is removed and the large stirrups are then cut into smaller stirrups of the appropriate width links (e.g. pre-bent open/closed stirrup). The advanced filament winding process can produce tailored FRP reinforcement with a tensile strength exactly where it is needed. Experimental studies by Lee et al. [13], [47] have proved that advanced filament winding forms the fibres in wide and thin cross sections suitable manufacturing of closed FRP stirrups. This method also allows for quick and accurate fabrication of reinforcement cages with consistent quality of material and uniform cross-section. This is because the winding system allows the internal radius of the bend to be tighter than for traditional open stirrups as the fibres do not need to slide over each other as is required when bending a straight pultruded bar before the resin polymerizes [48].

Shear reinforcement is often produced from pultruded bars prior to resin polymerization in form of circular, rectangular, and others such as spiral shaped stirrup [49]. A recent study [32] reported that prefabricated 3D FRP reinforcement cages produced using filament winding were successfully used in concrete elements. The manufacturing process of the 3D reinforcement FRP cage included wet and dry winding process. In the wet-winding process, each layer of fiber was impregnated with a two-component epoxy resin, squeezed with a polytetrafluorethylene tool to remove any excess, and wound around the mold. The stirrups were cured at room temperature for 72 hrs, prior to being demolded. In the dry winding process, the pre-preg tow was wound around the mold, before being packed in a vacuum bag and cured at 120°C for 4 hrs. The results obtained from tests on bent reinforcement showed that the use of wound CFRP instead of conventional circular CFRP stirrups offered advantages in terms of construction flexibility at more affordable costs, but it can also help mitigate the strength reduction at bent corners.

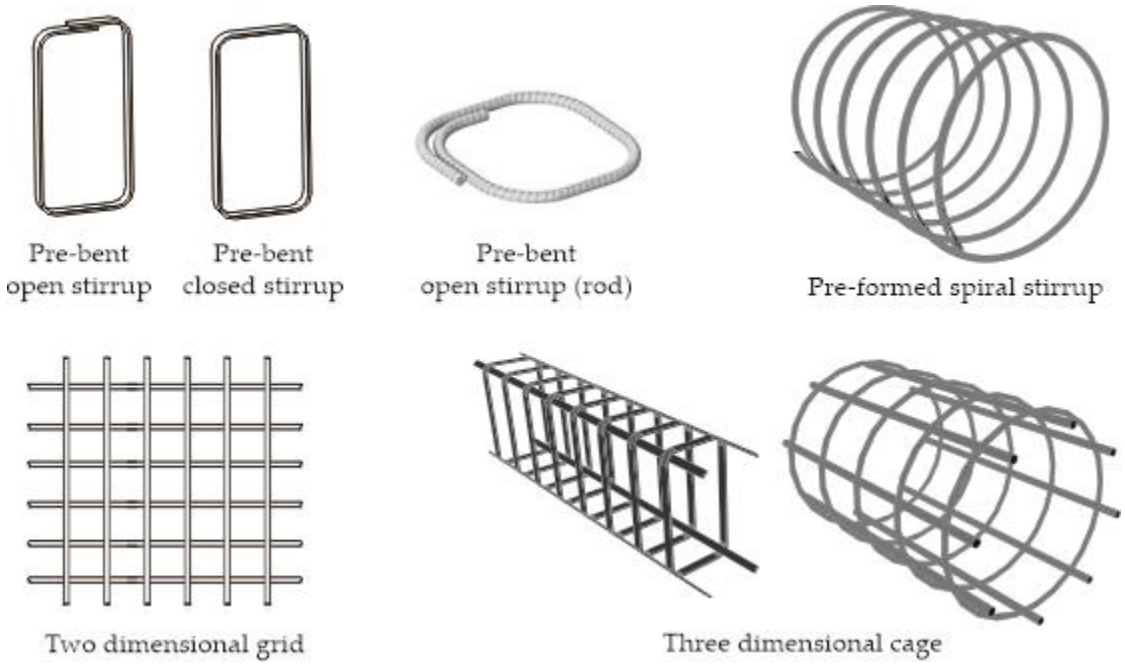

Figure 10. Various commercially available shaped FRP reinforcement (adopted from [6][48] [49] [32])

Based on the current advanced technology in producing complex 3D shaped FRP composites for engineering applications, yet it is remains the gap between the feasibility and durability of these engineering products to be used in the concrete structures over the design lifetime. Full-scale testing on both structural aspects as well as durability issues should be performed prior to fully exploit the full functionality of shaped FRP reinforcement in civil engineering application.

Due to the nature of which 3D-shaped FRP manufacturing and material anisotropic properties, advanced FEA should be used assessed the structural behavior when used as reinforcement in concrete elements.

7. Concluding Remarks

This paper presents an extensive review of the research works on the strength degradation in curved FRP composites and highlighted the performance of exiting predictive models for the bend capacity of FRP reinforcement. The use of FRP rebars as internal reinforcements for concrete,

however, is limited to specific structural elements and does not yet extend to the whole structure. The reasons for this relate to the limited availability of curved or shaped reinforcing elements on the market and their reduced structural performance. Various studies, in fact, have shown that the mechanical performance of bent portions of composite bars is reduced significantly under a multiaxial combination of stresses and that the tensile strength can be as low as 25% of the maximum tensile strength that can be developed in the straight part. The capacity of the bent specimens does not seem to vary linearly with the r/d ratio, as defined in the JSCE equation, and does not appear to be solely a function of the bend geometry. Rather, bond characteristics appeared to be important in controlling the development of stresses along the embedded portion of the composite and in dictating its ultimate behaviour. In a significant number of cases, the design provision according to JSCE's equation to predict bend capacity of FRP composites, however, were found to overestimate the bend capacity of FRP rebar with P/E ratios and SDs of up to 1.02 and 0.27, respectively. Recent practical predictive model based on the Tsai-Hill failure criteria by considering the material at marcromechanical level and the variability of the cross section along the bend predicted the experimental results more accurately (P/E=1.0) and with less scatter (SD=0.25) than the predictions of existing models.

It is worth remarking however, that none of the models considered in this analysis, including the macromechanical failure-based model, account for the influence of concrete strength, embedment length and tail length. These parameters are believed to play an important role in determining the behaviour of bent bars embedded in concrete and could be responsible for the large variation observed in the test data. Future research should be focused on the use of advanced finite element modelling to capture the true behaviour of unidirectional FRP composites at the micro level. This includes an input of the full definitions of material properties in both transversal and longitudinal directions. Biaxial tests on FRP composites should be performed in order to obtain the failure surface of the materials. Moreover, durability issues curved FRP reinforcement should be assessed for long term over the design lifetime. Advanced filament winding manufacturing process has been developed in which resin-impregnated fibres are wound onto specially designed mandrels to produce customized closed shapes and were used successfully as 3D reinforcement cage for concrete element. However, long-term durability should be further investigated before completely replacing internal steel reinforcement in concrete structures.

Acknowledgments: The author acknowledges the financial support by a TRF Mid-Career Research Scholarship. This project is partially supported by Thailand Toray Science Foundation through the Science & Technology Research Grants (STRG 2019).

Author Contributions: Thanongsak Imjai extensively researched the literature in the field and wrote the manuscript. Reyes Garcia conceived the article and executed the article editing. Maurizio Guadagnini and Kypros Pilakoutas suggested and supervised the work.

Funding: This research was funded by the Thailand National Research Disaster 2020 grant" and "The APC was funded by Thailand Toray Science Foundation through the Science & Technology Research Grants (STRG 2019)".

Conflicts of Interest: The authors declare no conflict of interest.

Abbreviations

The following abbreviations are used in this paper:

ACI	American Concrete Institute
AFRP	Aramid Fibre Reinforced Polymer
BS	British Standard
BSI	British Standard Institute
CEB	Comit Euro-international du Beton
CEN	Comite Europeen de Normalisation
CFCC	Carbon Fibre Composite Cable
CFRP	Carbon Fibre Reinforced Polymer
EC	Eurocode
FEA	Finite Element Analysis
FIB	Federation Interationale du Beton
FRP	Fibre Reinforced Polymer
GFRP	Glass Fibre Reinforced Polymer
ISE	Institution of Structural Engineering
ISIS	Intelligent Sensing for Innovative Structures
JSCE	Japanese Society of Civil Engineers
NFR	Non-Ferrous Reinforcement
OPC	Ordinary Portland Cement
RC	Reinforced Concrete
SLS	Service Limit State
ULS	Ultimate Limit State

115

Appendix : Bent test data from 1997 - 2017

Reference	No.	Type of FRP specimen	d (mm)	r (mm)	d_{fi} (mm)	r/d	r/d_{fi}	f_u (MPa)	f_b (MPa)	Eq. (1)	Eq. (2)	Eq. (3)		Eq. (4)	Eq. (5)	
												α =0.05	α =0.092		βset	βopt
JSCE [10]	1	Braided AFRP	8	16	8	2.0	2.0	1369	812	1110	840	548	663	698	952	463
	2		6	12	6	2.0	2.0	1142	796	926	700	457	553	582	794	387
	3		8	12	8	1.5	1.5	1369	846	1049	778	513	600	685	830	359
	4		10	12	10	1.2	1.2	1283	775	933	684	462	527	634	683	273
	5		6	12	6	2.0	2.0	1142	824	926	700	457	553	582	794	387
	6	7-stranded CFRP	8	16	8	2.0	2.0	1794	557	1455	1100	718	868	915	596	607
	7		6	12	6	2.0	2.0	1620	552	1314	994	648	784	826	538	548
	8		8	16	8	2.0	2.0	1794	595	1455	1100	718	868	915	596	607
	9		10	12	10	1.2	1.2	2271	553	1652	1211	818	932	1122	474	484
	10		6	12	6	2.0	2.0	1620	485	1314	994	648	784	826	538	548
Shehata et al. [14]	11	7-stranded CFRP	3.59	10.8	3.59	3.0	3.0	1782	916	1538	1201	802	1026	944	1199	838
	12		3.59	10.8	3.59	3.0	3.0	1782	1455	1538	1201	802	1026	944	1199	838
	13		4.4	13.2	4.40	3.0	3.0	1842	983	1590	1241	829	1061	976	1239	866
	14		4.4	13.2	4.40	3.0	3.0	1842	1187	1590	1241	829	1061	976	1239	866
	15		6.22	18.7	6.22	3.0	3.0	1875	1900	1618	1264	844	1080	994	1261	882
	16		6.22	18.7	6.22	3.0	3.0	1875	1421	1618	1264	844	1080	994	1261	882
	17		6.22	18.7	6.22	3.0	3.0	1875	798	1618	1264	844	1080	994	1261	882
	18	CFRP strip	5	15.0	5.00	3.0	3.0	1800	1242	1553	1213	810	1037	954	815	846
	19		5	15.0	5.00	3.0	3.0	1800	715	1553	1213	810	1037	954	815	846

Appendix : Bent test data from 1997 – 2017 *(cont.)*

Reference	No.	Type of FRP specimen	d (mm)	r (mm)	d_{fi} (mm)	r/d	r/d_{fi}	f_u (MPa)	f_b (MPa)	Eq. (1)	Eq. (2)	Eq. (3)		Eq. (4)	Eq. (5)	
												α =0.05	α =0.092		βset	βopt
Shehata et al. [14]	20	CFRP strip	5	35.0	5.00	7.0	7.0	1800	1163	1682	1413	1170	1699	1098	1350	1376
	21		5	35.0	5.00	7.0	7.0	1800	988	1682	1413	1170	1699	1098	1350	1376
	22		5	35.0	5.00	7.0	7.0	1800	858	1682	1413	1170	1699	1098	1350	1376
	23	GFRP	12	48.0	12.00	4.0	4.0	713	346	636	509	357	476	392	346	410
El-Sayed et al. [29]	24	CFRP rod	9.5	38.1	9.50	4.0	4.0	1328	701	1186	949	665	888	731	698	764
	25		9.5	38.1	9.50	4.0	4.0	1328	761	1186	949	665	888	731	698	764
	26		9.5	38.1	9.50	4.0	4.0	1328	656	1186	949	665	888	731	698	764
	27		9.5	38.1	9.50	4.0	4.0	1328	596	1186	949	665	888	731	698	764
	28		9.5	38.1	9.50	4.0	4.0	1328	789	1186	949	665	888	731	698	764
	29		12.7	50.8	12.70	4.0	4.0	1224	681	1093	874	612	818	673	643	703
	30		12.7	50.8	12.70	4.0	4.0	1224	539	1093	874	612	818	673	643	703
	31		12.7	50.8	12.70	4.0	4.0	1224	697	1093	874	612	818	673	643	703
Ahmed et al. [16]	32	CFRP rod	9.5	38	9.50	4.0	4.0	1538	712	1373	1099	769	1027	846	712	883
	33	GFRP rod	9.5	38	9.50	4.0	4.0	664	387	593	474	332	444	365	407	381
	34		15.9	63.6	15.90	4.0	4.0	599	404	535	428	300	400	329	367	344
	35		19.1	76.4	19.10	4.0	4.0	533	310	476	381	267	356	293	327	292
Lee et al. [13]	36	CFRP rod	9.5	42.8	9.50	4.5	4.5	1880	778	1698	1373	987	1343	1053	896	1161
	37		9.5	42.8	9.50	4.5	4.5	1880	1014	1698	1373	987	1343	1053	896	1161

Peer-reviewed version available at Polymers 2020, 12, 1653; doi:10.3390/polym12081653

Appendix : Bent test data from 1997 – 2017 *(cont.)*

Reference	No.	Type of FRP specimen	d (mm)	r (mm)	d_{fi} (mm)	r/d	r/d_{fi}	f_u (MPa)	f_b (MPa)	Eq. (1)	Eq. (2)	Eq. (3)		Eq. (4)	Eq. (5)	
												α =0.05	α =0.092		βset	βopt
Lee et al. [13]	38	CFRP strip	4	14.3	4.51	3.6	3.2	1850	763	1631	1293	886	1163	987	762	987
	39		4	14.3	4.51	3.6	3.2	1850	1012	1631	1293	886	1163	987	762	987
	40		4	28.5	4.51	7.1	6.3	1850	1102	1731	1456	1214	1768	1103	1224	1424
	41		4	28.5	4.51	7.1	6.3	1850	1192	1731	1456	1214	1768	1103	1224	1424
	42		4	42.8	4.51	10.7	9.5	1850	935	1769	1535	1545	1850	1220	1465	1604
	43		4	42.8	4.51	10.7	9.5	1850	1167	1769	1535	1545	1850	1220	1465	1604
	44		3	28.5	3.39	9.5	8.4	1740	1079	1654	1423	1349	1740	1111	1318	1466
	45		3	28.5	3.39	9.5	8.4	1740	1215	1654	1423	1349	1740	1111	1318	1466
	46		3	42.8	3.39	14.3	12.6	1740	1267	1682	1490	1763	1740	1258	1499	1589
	47		3	42.8	3.39	14.3	12.6	1740	1373	1682	1490	1763	1740	1258	1499	1589
	48		0.9	18	1.02	20.0	17.7	1880	1731	1835	1660	1880	1880	1550	1724	1782
	49		0.9	18	1.02	20.0	17.7	1880	1703	1835	1660	1880	1880	1550	1724	1782
	50		0.9	27	1.02	30.0	26.6	1880	1882	1849	1710	1880	1880	1880	1799	1827
	51		0.9	27	1.02	30.0	26.6	1880	1586	1849	1710	1880	1880	1880	1799	1827
Vint and Sheikh [6]	52	GFRP rod	9.43	51	9.43	5.4	5.4	833	555	764	628	475	664	481	701	568
	53		11.93	36	11.93	3.0	3.0	655	522	565	441	295	377	347	450	308
	54		13	23	13	1.8	1.8	912	531	721	540	353	420	461	457	275

Appendix : Bent test data from 1997 – 2017 *(cont.)*

Reference	No.	Type of FRP specimen	d (mm)	r (mm)	d_{fi} (mm)	r/d	r/d_{fi}	f_u (MPa)	f_b (MPa)	Eq. (1)	Eq. (2)	Eq. (3)		Eq. (4)	Eq. (5)	
												α =0.05	α =0.092		βset	βopt
Imjai et al. [6]	55	GFRP strip	3	6	3.39	2.0	1.8	720	236	584	442	288	348	364	227	244
	56		3	9	3.39	3.0	2.7	720	309	621	485	324	415	377	318	339
	57		3	12	3.39	4.0	3.5	720	324	643	514	360	481	389	393	414
	58		3	15	3.39	5.0	4.4	720	370	656	536	396	547	402	451	472
	59		3	9	3.39	3.0	2.7	720	316	621	485	324	415	377	318	339
	60		3	15	3.39	5.0	4.4	720	415	656	536	396	547	402	451	472
	61		3	9	3.39	3.0	2.7	720	340	621	485	324	415	377	318	339
	62		3	15	3.39	5.0	4.4	720	399	656	536	396	547	402	451	472
	63		3	9	3.39	3.0	2.7	720	367	621	485	324	415	377	318	339
	64		3	15	3.39	5.0	4.4	720	464	656	536	396	547	402	451	472
	65		3	9	3.39	3.0	2.7	720	299	621	485	324	415	377	318	339
	66		3	15	3.39	5.0	4.4	720	334	656	536	396	547	402	451	472
	67		3	9	3.39	3.0	2.7	720	324	621	485	324	415	377	318	339
	68		3	9	3.39	3.0	2.7	720	345	621	485	324	415	377	318	339
	69		3	6	3.39	2.0	1.8	720	183	584	442	288	348	364	227	244
	70		3	9	3.39	3.0	2.7	720	280	621	485	324	415	377	318	339
	71		3	12	3.39	4.0	3.5	720	301	643	514	360	481	389	393	414
	72		3	15	3.39	5.0	4.4	720	316	656	536	396	547	402	451	472
	73		3	9	3.39	3.0	2.7	720	281	621	485	324	415	377	318	339

Appendix : Bent test data from 1997 – 2017 *(cont.)*

Reference	No.	Type of FRP specimen	d (mm)	r (mm)	d_{fi} (mm)	r/d	r/d_{fi}	f_u (MPa)	f_b (MPa)	Eq. (1)	Eq. (2)	Eq. (3)		Eq. (4)	Eq. (5)	
												α =0.05	α =0.092		βset	βopt
Imjai et al. [6]	74	GFRP rod	9	54	9	6.0	6.0	760	611	703	583	456	648	448	494	545
	75		9	54	9	6.0	6.0	760	645	703	583	456	648	448	494	545
	76		9	54	9	6.0	6.0	760	592	703	583	456	648	448	494	545
	77		9	54	9	6.0	6.0	760	617	703	583	456	648	448	494	545
	78		13.5	54	13.5	4.0	4.0	590	382	527	422	295	394	325	296	339
	79		13.5	54	13.5	4.0	4.0	590	345	527	422	295	394	325	296	339
	80		9	54	9	6.0	6.0	760	419	703	583	456	648	448	494	545
Mean value (Prediction / Experiment)										*1.66*	*1.34*	*1.02*	*1.28*	*1.08*	*0.98*	*1.00*
Standard deviation (Prediction / Experiment)										*0.46*	*0.33*	*0.27*	*0.32*	*0.28*	*0.18*	*0.25*

Note: r is the internal bending radius, d is the nominal diameter (diameter for circular section and thickness for strip), d_{fi} is the transformed diameter, f_b is the experimental average failure stress, and f_u is the ultimate strength of the FRP bar.

References

[1] J. Plecnik and S. H. Ahmad, "Transfer of composite technology to design and construction of bridges," Final Rep. to USDOT, Contract No. DTRS 5683–C000043, 1988.

[2] A. Nanni, Antonio. De. Luca, and H. J. Zadeh, *Reinforced Concrete with FRP Bars: Mechanics and Design*. CRC Press, 2014.

[3] CurvedNFR, "Final report of the CRAFT RTD project CurvedNFR funded by the EU commission framework 5 GROWTH programme," Sheffield, United Kingdom, 2015.

[4] T. Ibell, A. Darby, and S. Denton, "Research issues related to the appropriate use of FRP in concrete structures," *Constr. Build. Mater.*, vol. 23, no. 4, pp. 1521–1528, 2009.

[5] British Standard Institution, *BS 8666:2005 Specification for scheduling, dimensioning, bending, and cutting of steel reinforcement for concrete*. BSI, London, UK., 2005.

[6] T. Imjai, M. Guadagnini, and K. Pilakoutas, "Bend strength of FRP bars: Experimental investigation and bond modeling," *J. Mater. Civ. Eng.*, vol. 29, no. 7, 2017, doi: 10.1061/(ASCE)MT.1943-5533.0001855.

[7] T. Imjai, M. Guadagnini, and K. Pilakoutas, "Curved FRP as concrete reinforcement," *Proc. Inst. Civ. Eng. Eng. Comput. Mech.*, vol. 162, no. 3, pp. 171–178, 2009, doi: 10.1680/eacm.2009.162.3.171.

[8] T. Maruyama, M. Honma, and H. Okamura, "Experimental Study on Tensile Strength of Bent Portion of FRP Rods," in *Non-Metallic (FRP) Reinforcement for Concrete Structures. Proceeding of 2nd RILEM symposium (FRPRCS-2)*, 1995, pp. 163–176.

[9] L. Vint and S. Sheikh, "Investigation of bond properties of alternate anchorage schemes for glass fiber-reinforced polymer bars," *ACI Struct. J.*, vol. 112, no. 1, pp. 59–68, 2015, doi: 10.14359/51687042.

[10] Japan Society of Civil Engineers, *Recommendation for Design and Construction of Concrete Structures using Continuous Fiber Reinforcing Materials*. Tokyo, Japan, 1997.

[11] M. R. Ehsani, H. Saadatmanesh, and S. Tao, "Bond of Hooked Glass Fiber Reinforced Plastic (GFRP) Reinforcing Bars to Concrete," *ACI Mater. J.*, vol. 122, no. 3, pp. 247–257, 1995.

[12] T. Nagasaka, H. Fukuyama, and M. Tanigaki, "Shear Performance of Concrete Beams Reinforced with FRP Stirrups," in *Proceedings of the International Symposium on Fibre Reinforced-Plastic Reinforcement for Concrete Structures*, 1995, pp. 789–811.

[13] C. Lee, M. Ko, and Y. Lee, "Bend strength of complete closed-type carbon fiber-reinforced polymer stirrups with rectangular section," *J. Compos. Constr.*, vol. 18, no. 1, pp. 1–11, 2014, doi: 10.1061/(ASCE)CC.1943-5614.0000428.

[14] E. Shehata, R. Morphy, and S. Rizkalla, "Fibre reinforced polymer shear reinforcement for concrete members: Behaviour and design guidelines," *Can. J. Civ. Eng.*, vol. 27, no. 5, pp. 859–872, 2000, doi: 10.1139/l00-004.

[15] K. Ishihara, T. Obara, Y. Sato, and Y. Kakuta, "Evaluation of ultimate strength of FRP rods at bent-up portion," in *Proceedings of the 3rd International Symposium on Non-Metallic (FRP) Reinforcement for Concrete Structures*, 1997, pp. 27–34.

[16] E. A. Ahmed, A. K. El-Sayed, E. El-Salakawy, and B. Benmokrane, "Bend strength of FRP stirrups: Comparison and evaluation of testing methods," *J. Compos. Constr.*, vol. 14, no. 1, pp. 3–10, 2010, doi: 10.1061/(ASCE)CC.1943-5614.0000050.

[17] H. Nakamura and I. Higai, "Evaluation of Shear Strength on Concrete Beams Reinforced with FRP," *Concr. Libr. JSCE*, vol. 26, pp. 111–123, 1995.

[18] R. Morphy, E. Sheata, and S. Rizkalla, "Bent Effect on Strength of CFRP StirrupsBent Effect on Strength of CFRP Stirrups," in *In 3rd International Symposium on Non-Metallic (FRP) Reinforcement for Concrete*

Structures, 1997, pp. 19–26.

[19] A. G. Razaqpur and S. Spadea, "Shear Strength of FRP Reinforced Concrete Members with Stirrups," *J. Compos. Constr. ASCE*, vol. 19, no. 1, 2015.

[20] ACI 440.1R-15, *Guide for the design and construction of concrete reinforced with FRP bars*. American Concrete Institute (ACI), Farmington Hills, MI, USA., 2015.

[21] ISIS M03-01, *Reinforcing concrete structures with fibre reinforced polymers*. Design Manual No. 3, Canadian Network of Centres of Excellence on Intelligent Sensing for Innovative Structures, Winnipeg., 2001.

[22] Fib Bulletin 40, "FRP reinforcement in concrete structures," *Int. Fed. Struct. Concr.*, 2007.

[23] T. Imjai, M. Guadagnini, K. Pilakoutas, R. Garcia, P. Sukontasukkul, and S. Limkatanyu, "A practical macro-mechanical model for the bend capacity of fibre-reinforced polymer bars," *Proc. Inst. Civ. Eng. - Struct. Build.*, 2020, doi: 10.1680/jstbu.19.00135.

[24] K. Ozawa, K. Sekijima, and H. Okamura, "Flexural Fatigue Bahaviour of Concrete Beams with FRP Reinforcemen," *Trans. Japanese Concr. Inst.*, vol. 9, pp. 289–296, 1987.

[25] S. Miyata, S. Tottori, T. Terada, and K. Sekijima, "Experimental study on tensile strength of FRP bent bar," *Trans. Japanese Concr. Inst.*, vol. 11, pp. 185–191, 1989.

[26] S. Mochizuki, Y. Matsuzaki, and M. Sugita, "Evaluation Items and Methods of FRP Reinforcement as Structural Element," *Trans. Japanese Concr. Inst.*, vol. 11, pp. 117–131, 1989.

[27] ACI Committee 440, "Guide for the Design and Construction of Structural Concrete Reinforced with Firber-Reinforced Polymer (FRP) Bars (ACI 440.1R-15)," *American Concrete Institute*. 2015, doi: 10.1016/0011-7471(75)90030-3.

[28] T. Imjai, M. Guadagnini, R. Garcia, and K. Pilakoutas, "A practical method for determining shear crack induced deformation in FRP RC beams," *Eng. Struct.*, vol. 126, 2016, doi: 10.1016/j.engstruct.2016.08.007.

[29] A. K. El-Sayed, E. El-Salakawy, and B. Benmokrane, "Mechanical and structural characterization of new carbon FRP stirrups for concrete members," *J. Compos. Constr.*, vol. 11, no. 4, pp. 352–362, 2007, doi: 10.1061/(ASCE)1090-0268(2007)11:4(352).

[30] T. Ueda, Y. Sato, Y. Kakuta, A. Imamura, and H. Kanematsu, "Failure Criteria for FRP rods Subjected to a Combination of Tensile and Shear Forces," in *Non-Metallic (FRP) Reinforcement for Concrete Structures. Proceeding of 2nd RILEM symposium (FRPRCS-2)*, 1995, pp. 26–33.

[31] J. Liu, Y. Zhao, Y. Yang, and Y. F. Chen, "Bending Capacity and Elastic Stiffness for a Novel Configuration of Cold-Formed U-Shaped Steel-and-Concrete Composite Beams," *J. Struct. Eng. (United States)*, vol. 145, no. 10, pp. 1–12, 2019, doi: 10.1061/(ASCE)ST.1943-541X.0002394.

[32] S. Spadea, J. Orr, A. Nanni, and Y. Yang, "Wound FRP Shear Reinforcement for Concrete Structures," *J. Compos. Constr.*, vol. 21, no. 5, 2017, doi: 10.1061/(ASCE)CC.1943-5614.0000807.

[33] H. M. Mohamed, A. H. Ali, and B. Benmokrane, "Behavior of Circular Concrete Members Reinforced with Carbon-FRP Bars and Spirals under Shear," *J. Compos. Constr.*, vol. 21, no. 2, pp. 1–12, 2017, doi: 10.1061/(ASCE)CC.1943-5614.0000746.

[34] H. M. Mohamed, O. Chaallal, and B. Benmokrane, "Torsional moment capacity and failure mode mechanisms of concrete beams reinforced with carbon FRP bars and stirrups," *J. Compos. Constr.*, vol. 19, no. 2, pp. 1–10, 2015, doi: 10.1061/(ASCE)CC.1943-5614.0000515.

[35] A. K. El-Sayed and K. Soudki, "Evaluation of shear design equations of concrete beams with FRP reinforcement," *J. Compos. Constr.*, vol. 15, no. 1, pp. 9–20, 2011, doi: 10.1061/(ASCE)CC.1943-5614.0000158.

[36] E. A. Ahmed, E. F. El-Salakawy, and B. Benmokrane, "Shear performance of RC Bridge girders reinforced with carbon FRP stirrups," *J. Bridg. Eng.*, vol. 15, no. 1, pp. 44–54, 2010, doi:

10.1061/(ASCE)BE.1943-5592.0000035.

[37] H. El Chabib and M. Nehdi, "Shear capacity of FRP stirrups in FRP-reinforced concrete beams based on genetic algorithms approach," *Proc. 2008 Struct. Congr. - Struct. Congr. 2008 Crossing Borders*, vol. 314, pp. 1–9, 2008, doi: 10.1061/41016(314)53.

[38] I. Currier, C. Fogstad, D. Walrath, and C. Dolan, "Bond Development of Thermoplastic FRP Shear Reinforcement Stirrups," in *Proceedings of the Third Materials Engineering Conference, ASCE*, 1994, pp. 592–597.

[39] ACI Committee 440, "Guide Test Methods for Fiber- Reinforced Polymer (FRP) Composites for Reinforcing or Strengthening Concrete and Masonry Structures," *ACI 440.3R-04*. 2012.

[40] ACI 318-14, *Building code requirements for structural concrete*. American Concrete Institute, Farmington Hills, MI, USA., 2014.

[41] X. Yang, J. Wei, A. Nanni, and L. R. Dharani, "Shape Effect on the Performance of Carbon Fiber Reinforced Polymer Wraps," *J. Compos. Constr. ASCE*, vol. 8, no. 5, pp. 444–451, 2004.

[42] ISIS, *Specifications for product certification on fibre reinforced polymers (FRPs) as internal reinforcement in concrete structures*, Product ce. Univ. of Manitoba, Winnipeg, MB, Canada, 2006.

[43] ACI 440.6M-08, *Specification for carbon and glass fiber-reinforced polymer bar materials for concrete reinforcement*. Farmington Hills, MI., 2008.

[44] K. Pilakoutas, M. Guadagnini, K. Neocleous, and S. Matthys, "Design guidelines for FRP reinforced concrete structures," *Proc. Inst. Civ. Eng. – Struct. Build.*, vol. 164, no. 4, pp. 255–263, 2011.

[45] ISIS-M03-07, *Reinforcing concrete structures with fiber reinforced polymers*. Univ. of Winnipeg, Winnipeg, MB, Canada., 2007.

[46] Hwai-Chung. Wu and Christopher. D. Eamon, *Strengthening of Concrete Structures using Fiber Reinforced Polymers (FRP). Design, Construction and Practical Applications*. Woodhead Publishing, 2017.

[47] C. Lee, S. Lee, and S. Shin, "Shear Capacity of RC Beams with Carbon Fiber- 464 Reinforced Polymer Stirrups with Rectangular Section," *J. Compos. Constr.*, vol. 20, no. 4, 2016.

[48] T. Imjai, M. Guadagnini, and K. Pilakoutas, "Curved FRP as concrete reinforcement," *Proc. Inst. Civ. Eng. Eng. Comput. Mech.*, vol. 162, no. 3, 2009, doi: 10.1680/eacm.2009.162.3.171.

[49] A. Ali, H. Mohamed, and B. Benmokrane, "Shear behavior of circular concrete members reinforced with GFRP bars and spirals at shear span-to-depth ratios between 1.5 and 3.0," *J. Compos. Constr.*, 2016.